Proc. Natl. Acad. Sci. USA
Vol. 86, pp. 1698–1702, March 1989
Neurobiology

Stimulus-specific neuronal oscillations in orientation columns of cat visual cortex

(thalamus/area 17)

CHARLES M. GRAY AND WOLF SINGER

Max Planck Institute for Brain Research, Deutschordenstrasse 46, 6000 Frankfurt am Main 71, Federal Republic of Germany

Communicated by David H. Hubel, November 28, 1988

ABSTRACT **In areas 17 and 18 of the cat visual cortex the firing probability of neurons, in response to the presentation of optimally aligned light bars within their receptive field, oscillates with a peak frequency near 40 Hz. The neuronal firing pattern is tightly correlated with the phase and amplitude of an oscillatory local field potential recorded through the same electrode. The amplitude of the local field-potential oscillations are maximal in response to stimuli that match the orientation and direction preference of the local cluster of neurons. Single and multiunit recordings from the dorsal lateral geniculate nucleus of the thalamus showed no evidence of oscillations of the neuronal firing probability in the range of 20–70 Hz. The results demonstrate that local neuronal populations in the visual cortex engage in stimulus-specific synchronous oscillations resulting from an intracortical mechanism. The oscillatory responses may provide a general mechanism by which activity patterns in spatially separate regions of the cortex are temporally coordinated.**

The mechanism by which populations of neurons in the cerebral cortex temporally coordinate their activity patterns in response to specific sensory stimuli constitutes a basic unresolved question in sensory physiology. In the vertebrate olfactory system the spatiotemporal coordination of neuronal activity is achieved by the synchronization of oscillatory responses having a frequency in the range of 40–80 Hz (1–5). Evidence suggesting that a similar mechanism for the synchronization of activity may operate in the neocortex has come from field potential recordings in awake animals. It has been demonstrated that oscillatory activity in the high beta-frequency range (20–50 Hz) occurs in sensory areas of the neocortex when the animals direct their attention to meaningful stimuli (6–11).

Previously we have discovered, from recordings in area 17 of awake kittens, that neuronal responses recorded during periods of behavioral attention exhibit a rhythmic firing pattern that is tightly correlated with an oscillatory local field potential (LFP) having a frequency near 40 Hz (12). Thus, we sought to determine whether the oscillatory responses could also be recorded under varying conditions of anesthesia that would permit a more quantitative analysis of both their stimulus specificity as well as their temporal properties. Here, we extend our previous observations (13) and report that local groups of neurons, within functional columns of the visual cortex, engage in stimulus-specific oscillatory responses having a frequency near 40 Hz. This periodic neuronal activity is tightly correlated to the simultaneously recorded LFP, which in the majority of recordings has a similar orientation and direction preference as the local cluster of neurons. No comparable oscillations of firing probability were found for the thalamic input to visual cortex, indicating that the generation of oscillatory responses is a cortical phenomenon. The results suggest the hypothesis that the temporal pattern of the oscillatory response is used to synchronize the activity of neuronal populations in spatially separate regions of the cortex.

The publication costs of this article were defrayed in part by page charge payment. This article must therefore be hereby marked "*advertisement*" in accordance with 18 U.S.C. §1734 solely to indicate this fact.

MATERIALS AND METHODS

Experiments were performed on a total of 15 adult cats and 12 kittens 4–6 weeks of age. The experimental procedures for preparation of the animals, the presentation of visual stimuli, and the recording of neuronal responses in the visual cortex have been described (14). For surgery anesthesia was induced by injection of a short-acting anesthetic (ketamine at 15 mg/kg or hexobarbital at 15 mg/kg). During recording, anesthesia was maintained with a mixture of 30% O_2/70% N_2O, supplemented by 0.1–0.3% halothane or hexobarbital (5 mg/kg). Recordings usually began 3–5 hr after the initial anesthesia to insure that the effects of ketamine, when used, had worn off. The wound edges were infiltrated with lidocaine. Muscle paralysis was achieved by a continuous i.v. infusion of hexocarbacholinbromide (Imbretil).

Multiunit activity (MUA) and LFPs were recorded from one to five 25-μm diameter Teflon-coated platinum–iridium electrodes whose tips were etched to a point and coated with platinum black (15). The LFP and MUA were differentially amplified (5000–20,000 and 5000, respectively) and filtered (1–100 Hz and 1–3 kHz, respectively). The output of the MUA amplifier was fed through a threshold detector to isolate units, on the average, at twice the noise level, and the LFP and Schmitt trigger output were digitized on separate channels at a rate of 1 kHz each. The receptive field properties of the MUA recorded from each electrode were assessed with light stimuli projected on a tangent screen located 1.12 m in front of the cat's eye plane. All stimulus trials were 10 sec in duration, and trial sets were composed of 10 trials to each stimulus. On each trial the light stimulus was on and moving over the receptive field first in one direction (first through fourth sec) and then in the other direction (sixth through ninth sec). For histological verification of the electrode tip locations DC currents (5–10 μA for 20 sec) were applied to the electrodes at the end of measurements, and the lesion locations were retrieved in Nissl-stained sections of the perfused fixed brains.

A sample of the data, to be used for quantitative analysis, was taken from 30 recording sites in areas 17 and 18 of 14 animals. In four of the adult cats recordings of single and multiunit activity were also made in the dorsal lateral geniculate nucleus of the thalamus. In 25 recordings from area 17 a quantitative assay of orientation selectivity was performed at angular intervals of 22.5°.

Four separate sets of calculations were performed on the data to examine the temporal properties of the MUA and LFP

Abbreviations: LFP, local field potential; MUA, multiunit activity; ACF, autocorrelation function.

responses and the relationship between the two signals: the autocorrelation function (ACF) of the MUA, the power spectrum of the fast Fourier transform of the LFP, the spike-triggered average of the LFP, and the orientation tuning curves of both the MUA and the LFP.

Multiunit histogram tuning curves were computed by counting the number of spikes within a 1-sec interval centered on the peak of the response. Tuning curves of the LFP amplitudes were computed by integrating the average power spectrum within a frequency range of 25–65 Hz. This choice of frequency range was based on the finding that the average peak frequency of the stimulus-evoked LFP was near 40 Hz. Power spectra were computed on each trial from data samples of 1-sec duration taken at a latency of 0 sec for control and at latencies centered on the peak of the multiunit responses for both directions of stimulus movement.

For calculating the spike-triggered averages of the LFP the signals were first divided into two 5-sec epochs for each direction of stimulus movement and then digitally bandpass-filtered at 20–80 Hz to retain only the stimulus-evoked frequency components. The resultant distributions of voltage values were then normalized to their Z scores by subtracting the mean and dividing by the standard deviation (SD) of the LFP voltages recorded during each epoch. Each occurrence of a spike in the signal filtered for multiunit recording was then used as a trigger point to compute the average distribution of the LFP voltage ± 50 msec in time centered on the occurrence of the spikes. The resultant spike-triggered averages were expressed in units of the SD of the LFP voltage at a resolution of 0.1 SD.

To further reveal the temporal structure of the LFP responses a finer grained spectral analysis was performed on selected sets of individual trials. The LFP signal from each trial was subdivided into forty 256-msec epochs, and the power spectrum was computed for each epoch. The resulting set of 40 power spectra were displayed as a compressed spectral array for each trial.

RESULTS

A typical response of both the MUA and LFP recorded from area 17 in an adult cat is shown in Fig. 1*A*. When a light bar of optimal orientation, velocity, and preferred direction of movement was passed through the receptive field of the recorded neurons we consistently observed a rhythmic firing pattern in the neuronal spike train that was associated with a high-amplitude oscillation of the LFP. Close examination of the records revealed that the spikes occurred during the negative phase of the LFP oscillations (Fig. 1*A*, lower two traces). Computation of the power spectra of the LFPs demonstrated that the oscillatory activity was clearly stimulus-dependent (Fig. 1*C*). In the absence of a sensory stimulus in the receptive field the spontaneous activity of the neurons was associated with large amplitude fluctuations of the LFP in the frequency range of 1–10 Hz. The presentation of an optimal stimulus in the receptive field evoked a broad

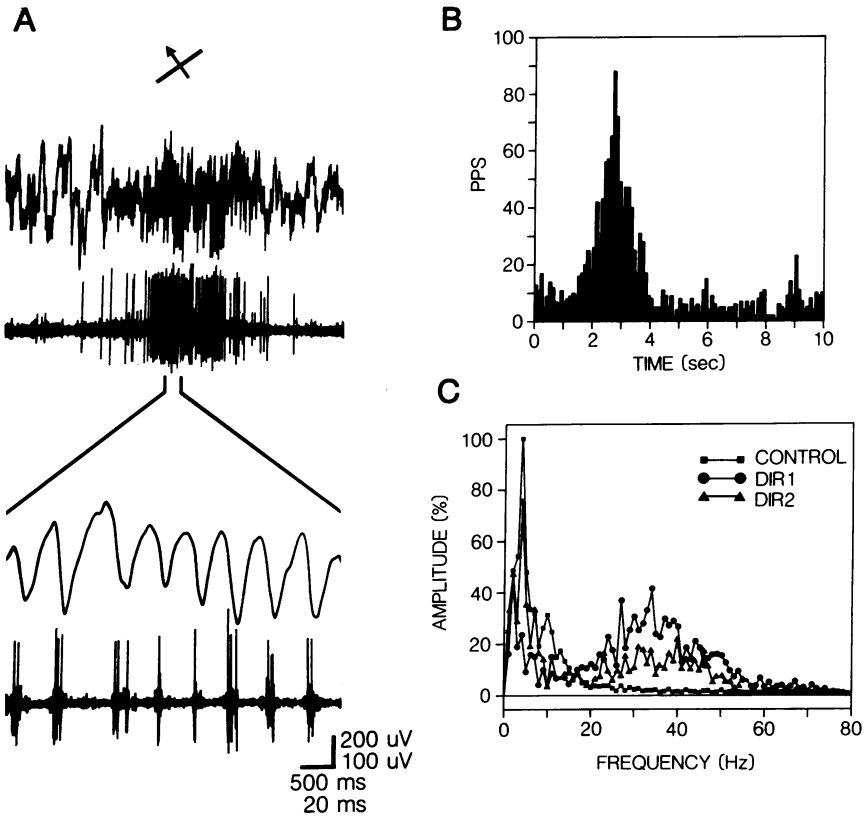

FIG. 1. MUA and LFP responses recorded from area 17 in an adult cat to the presentation of an optimally oriented light bar moving across the receptive field. (*A*) Oscilloscope records of a single trial showing the response to the preferred direction of movement. In the upper two traces, at a slow time scale, the onset of the neuronal response is associated with an increase in high-frequency activity in the LFP. The lower two traces display the activity at the peak of the response at an expanded time scale. Note the presence of rhythmic oscillations in the LFP and MUA (35–45 Hz) that are correlated in phase with the peak negativity of the LFP. Upper and lower voltage scales are for the LFP and MUA, respectively. (*B*) Poststimulus time histogram of the MUA recorded over 10 trials illustrating a clear directional preference (PPS, pulses per second). (*C*) Average LFP frequency spectra computed from 1-sec data epochs (1024 points) over 10 trials at three separate latencies after the onset of each trial [control = 0 sec, direction 1 (DIR1) = 2.2 sec, direction 2 (DIR2) = 7.0 sec]. The LFP signals were digitally lowpass-filtered at 80 Hz. As the stimulus passes through the receptive field there is a simultaneous reduction of low frequencies and an increase in amplitude of high frequencies in the LFP that is more pronounced for the preferred direction of movement.

spectrum increase in the amplitude of the LFP (Fig. 1C), which, on the average, ranged from 25 to 65 Hz. However, the stimulus-dependent increase in the LFP amplitude often exhibited a different degree of specificity when compared with the simultaneously recorded unit response (compare Fig. 1 B and C).

We recorded similar oscillatory responses in each cat throughout areas 17 and 18, with varying amplitude and frequency, at all cortical depths and with equal probability in both adult cats and kittens. The occurrence of the oscillatory responses was neither dependent on the initial anesthesia, provided that we waited for the ketamine to wear off, nor on the anesthetics used for the maintenance of anesthesia. Across subjects and recording locations the average peak frequency of the LFP evoked by a light stimulus of optimal orientation, direction of movement, and velocity was 42 ± 7 Hz (n = 140).

This latter finding, combined with our observations of the raw data as shown in Fig. 1A, suggested that during brief periods of the response (200–500 msec), when the amplitude of the LFP oscillations was maximal, the frequency was restricted to a narrow range of approximately 35–50 Hz. To test this hypothesis we calculated the frequency spectra of short epochs of the LFP (256 msec) on individual trials and compared the time course of the neuronal response (Fig. 2A) with that observed in the LFP. An example of the results is shown in Fig. 2B in the form of a compressed spectral array. The data are taken from area 17 of a 5-week-old kitten, and the low- and high-frequency components have been removed using a digital bandpass filter (20–80 Hz). By comparing parts A and B in Fig. 2 it can be seen that both the amplitude and latency of the responses are similar for the LFP and the MUA. The peak of the oscillatory response recorded in the LFP is limited to a narrow frequency range (38 ± 4 Hz) and lasts for a duration not exceeding 250 msec in the forward direction and 500 msec in the reverse direction. In addition, the frequency distribution and time of occurrence of the peak amplitude observed in the LFP was never twice the same on successive trials. This variation of response latency and frequency content contributed to the broad band frequency distribution observed in the average LFP power spectrum computed over 10 trials (Fig. 1C).

A confirmation of this finding was obtained by computing both the autocorrelation function (ACF) of the MUA and the spike-triggered average of the LFP (Fig. 2 C and D). A clear periodicity appeared in the ACF in 14 out of 30 recordings. In each of the 14 cases the frequency of the ACF matched that of the peak frequency in the corresponding LFP power spectrum (Fig. 2 B and C). Recomputation of the ACF after shuffling the trial sequence (i.e., shift predictor) completely eliminated any periodicity in the ACF, thus demonstrating that the rhythmic firing pattern in the spike train is not synchronized from one trial to the next (Fig. 2C, bottom two traces). In addition, computation of the spike-triggered average of the LFP yielded an oscillatory waveform of the same frequency as the peak in the power spectrum in 29 out of 30 cases (Fig. 2D). On the average the spikes occurred during the peak negativity of the LFP oscillation with an average phase relation of 0.4 ± 1.9 msec. In each case recomputation of the spike-triggered average, after shifting the two time

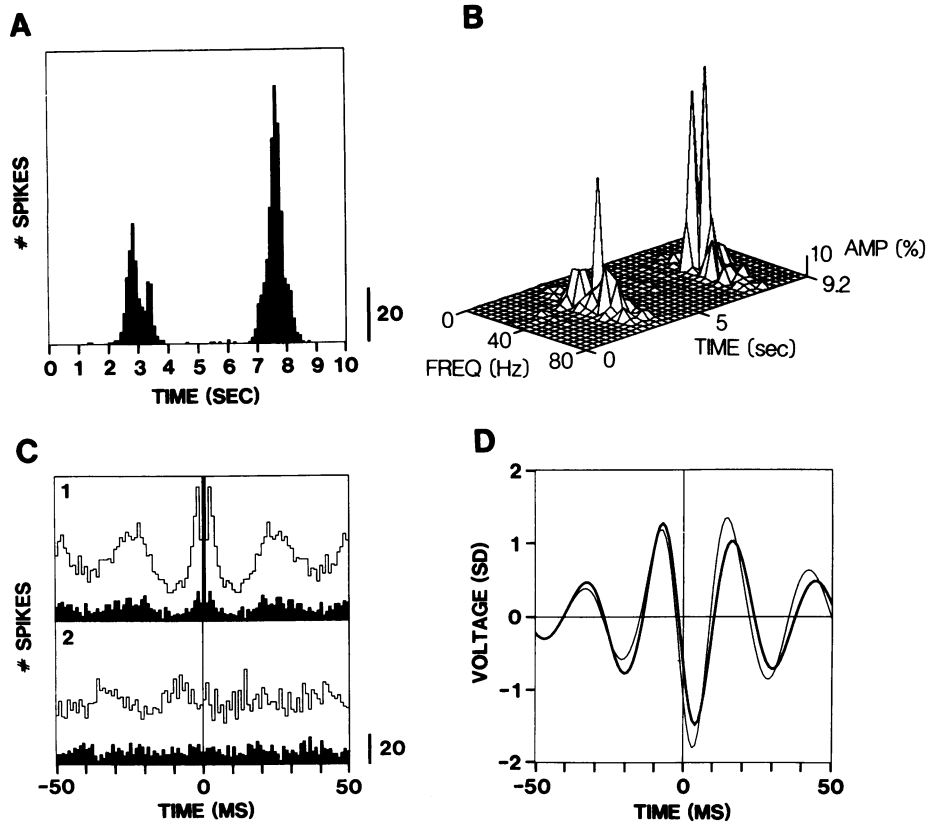

FIG. 2. Temporal properties of the MUA and LFP responses recorded from area 17 in a 5-week-old kitten. (A) Poststimulus time histogram of the MUA. (B) Distribution of the LFP amplitude versus frequency and time on a single trial recorded from the same electrode in which the MUA was sampled. The frequency resolution is 4 Hz, and the temporal resolution is 256 msec. The amplitude scale is expressed as a fractional percentage of the peak amplitude. (C1) ACFs of the same MUA recorded in A displayed for both the forward (filled bars) and the reverse (unfilled bars) direction of stimulus movement. Note the rhythmic firing pattern with a period length near 25 msec for both directions of stimulus movement. (C2) Recomputation of the ACF after shuffling the trial sequence by one stimulus period (i.e., shift predictor). (D) Normalized spike-triggered average of the LFP for both the forward (thick line) and the reverse (thin line) directions of stimulus movement. Results are expressed in units of SD of the LFP voltage recorded during each direction of movement.

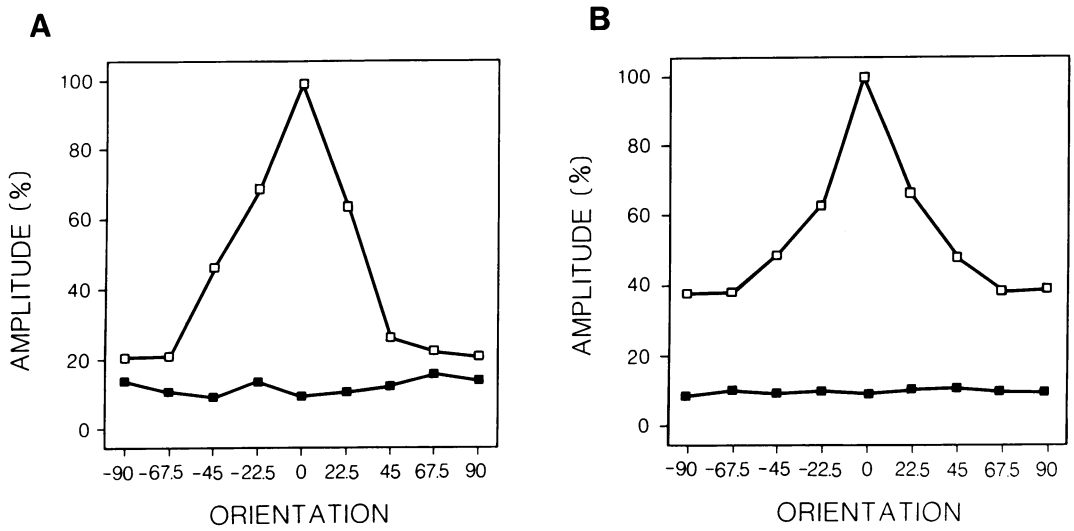

FIG. 3. Average tuning curves of the MUA (*A*) and LFP power spectrum amplitude (*B*) for responses to the optimal direction of stimulus movement (□) and the spontaneous activity occurring at the onset of each trial (■). Each graph represents the normalized average computed from the 14 recordings in which the orientation tuning and directional preference of the LFP matched that of the MUA. The orientation axis is referenced to that angle at which a maximal response was observed for each recording; orientation angles are displayed at intervals of 22.5° with respect to optimal.

series relative to each other by 200 msec, completely eliminated the correlation (data not shown), thereby demonstrating that the relation is not a frequency-dependent effect. A preliminary analysis of data obtained with conventional single-cell recording revealed that oscillatory responses occur much more frequently in cells with complex than in cells with simple receptive fields.

Further information on the spatial distribution and stimulus specificity of the LFP oscillations was obtained by computing orientation tuning curves for both the MUA and the LFP power spectra in the range of 25–65 Hz. In 14 of 25 recordings the ampitude of both the LFP oscillations and the MUA responses exhibited a similar preference for the orientation and direction of movement of the stimulus. In the remaining 11 recordings the stimulus-induced LFP oscillations exhibited either no orientation or directional preference or their preferences did not match those of the MUA. Fig. 3 illustrates the average orientation tuning curves at the preferred direction of stimulus movement for both the MUA and the LFP for the 14 matched recordings. The tuning is similar within an angle of ± 30° from the optimal orientation, but at larger angles the LFPs show a broader tuning than the MUA. The peak frequency of the LFP responses, however, did not vary significantly as a function of either the orientation or the direction of stimulus movement.

In four cats we examined the possible contribution of thalamic oscillatory input on the cortical responses. We recorded both single and multiple unit responses in the A, A1, and C laminae of the lateral geniculate nucleus of the thalamus to the presentation of stimuli optimized separately for thalamic and cortical responses. In no case did we observe oscillations of the neuronal firing probability in the range of 20–70 Hz.

DISCUSSION

In summary these findings suggest three conclusions: (*i*) During responses to light stimuli adjacent neurons have a strong tendency to be active simultaneously and in synchrony. Nonsynchronous neuronal firing would not be expected to produce a periodic ACF, a high-amplitude oscillatory LFP, and to yield a consistent relationship between firing probability and the LFP polarity and amplitude. (*ii*) The neuronal oscillations result from intracortical mechanisms and are not driven by oscillatory thalamic input. (*iii*) Neurons actively involved in the generation of the oscillations are restricted to a small volume of cortical tissue confined approximately to a single orientation column. This conclusion is supported by the similarity of the orientation tuning between the LFP and MUA responses.

These results taken together suggest that the synchronous oscillation of an ensemble of coactive neurons in the frequency range of 35–50 Hz is an integral part of the neuronal response in the visual cortex. The oscillatory responses are not an artifact of the preparation, the recording geometry, or the level of anesthesia. We have observed these responses in awake kittens (12) and over a large range of anesthesia levels and under different types of anesthesia. Moreover, the oscillatory neuronal responses exhibit the same degree of stimulus specificity as reported in the literature for single-cell responses. What is unclear, however, is the failure on 16 out of 30 cases to observe a rhythmicity in the ACF of the MUA even when these responses were recorded during a high-amplitude stimulus-evoked oscillation of the LFP (29 out of 30). These results may have several explanations: (*i*) The firing pattern of many neurons in the cortex may be truly nonrhythmic, in which case only a selected number of observations would reveal the rhythmicity. Indeed our initial observations confirmed that oscillatory responses occur preferentially in complex cells. (*ii*) The range of firing frequencies of neurons may overlap and have differing degrees of frequency variation (16). Such an effect would be expected to average out any rhythmicities seen over many observations, thereby resulting in a nonrhythmic ACF. (*iii*) Computation of the ACF may combine periods of spontaneous activity with brief periods of rhythmic and nonrhythmic firing during a response. In this case a nonrhythmic ACF would be expected if the periods of nonrhythmic firing greatly exceeded the duration of the oscillatory responses. The finding that the peak amplitude of the oscillation observed in the LFP lasts for periods as short as 200–300 msec supports this interpretation.

The electrogenic source of the LFP clearly resides in the cortex. However, even though the LFP oscillations were observed in 29 out of 30 cases analyzed quantitatively, in 11 of 25 cases the stimulus specificity of the LFP did not match that of the underlying unit activity. This finding suggests that the local source and sink currents generating the LFP reflect

activity in a larger population of cells than that sampled by the multiunit electrodes. In many cases, however, there is a tight coupling of the stimulus specificity of the two signals, and this coupling is reflected in the greatly increased firing probability of the neurons during the negative phase of the LFP oscillation (Fig. 2). What deserves emphasis is that the field potential has revealed the oscillatory behavior of the neuronal responses and because of its close correlation to the MUA this field potential must reflect the synchronous activity of a population of cells. Thus, in a limited number of recordings the field potential may serve as a useful signal for analyzing the temporal dynamics of interacting populations of cells.

Although the mechanisms underlying the generation of the oscillatory activity are largely unknown, a qualitative comparison to the olfactory bulb and cortex (2–4, 17, 18) suggests that the interaction among a population of synaptically coupled neurons exhibiting both mutual excitation and recurrent inhibition are sufficient for the generation of oscillations (19–23). Simulation studies of both the olfactory system (18) and the visual cortex (19, 23) have demonstrated that neural networks constructed using this basic scheme readily generate oscillatory activity, the frequency of the oscillation being determined by the transmission time required to traverse the inhibitory feedback loop (18). This interpretation could provide one possible explanation for the data of Ferster (24), who demonstrated that the occurrence of both inhibitory and excitatory postsynaptic potentials were maximal at optimal orientations. These results would be expected if the oscillatory activity resulted from both mutual excitation and recurrent inhibition within a local population of neurons. Furthermore, close examination of the intracellular recordings of Ferster (ref. 24, see figures 3 and 4 therein) reveals that at optimal orientations the inhibitory postsynaptic potential activity occurs rhythmically with a frequency near 40 Hz, thus supporting the above interpretation.

In conclusion, our results show that groups of adjacent cortical neurons, when activated appropriately, engage in cooperative interactions as postulated on theoretical grounds previously (25, 26). Our results demonstrate further that these interactions lead to coherent and periodic patterns of activity, suggesting that the phase of the oscillatory response may be used as a further dimension of coding in addition to the amplitude and duration of the response. One role for this temporal code would be to enable columns of cells in different parts of the cortex, representing different parts of the visual field, to synchronize their respective activity patterns. Results obtained recently with multielectrode recordings indicate that such synchronization across spatially separate columns does occur (refs. 27, 28, and C.M.G., P. König, A. K. Engel, W.S., unpublished work).

We thank Christa Ziegler for assistance in preparation of the electrodes and Alexa Franke for the histological processing.

1. Adrian, E. D. (1950) *Br. Med. Bull.* **6,** 330–333.
2. Freeman, W. J. (1975) *Mass Action in the Nervous System* (Academic, New York).
3. Freeman, W. J. (1987) in *Handbook of Electroencephalography and Clinical Neurophysiology*, eds. Gevins, A. & Remond, A. (Elsevier, Amsterdam), Vol. 3A, Part 2, Chap. 14.
4. Gray, C. M. & Skinner, J. E. (1988) *Exp. Brain Res.* **69,** 378–386.
5. Vianna Di Prisco, G. & Freeman, W. J. (1985) *Behav. Neurosci.* **99,** 964–978.
6. Lopes Da Silva, F. H., van Rotterdam, A., Storm van Leeuwen, W. & Tielen, A. M. (1970) *Electroencephalogr. Clin. Neurophysiol.* **29,** 260–268.
7. Rougeul, A., Bouyer, J. J., Dedet, L. & Debray, O. (1979) *Electroencephalogr. Clin. Neurophysiol.* **46,** 310–319.
8. Bouyer, J. J., Montaron, M. F. & Rougeul, A. (1981) *Electroencephalogr. Clin. Neurophysiol.* **51,** 244–252.
9. Bouyer, J. J., Montaron, M. F., Vahnee, M. P., Albert, M. P. & Rougeul, A. (1987) *Neuroscience* **22,** 863–869.
10. Freeman, W. J. & van Dijk, B. W. (1987) *Brain Res.* **422,** 267–276.
11. Sheer, D. E., Kaufman, P. & DeFrance, T. (1988) *J. Physiol. Behav.*, in press.
12. Gray, C. M. & Singer, W. (1987) *Neuroscience* **22,** Suppl. S434.
13. Gray, C. M. & Singer, W. (1987) *Soc. Neurosci. Abstr.* 404.3.
14. Greuel, J. M., Luhmann, H. J. & Singer, W. (1987) *Dev. Brain Res.* **34,** 141–149.
15. Mioche, L. & Singer, W. (1988) *J. Neurophysiol.*, in press.
16. Rose, D. (1979) *Exp. Brain Res.* **37,** 595–604.
17. Haberly, L. B. & Bower, J. M. (1984) *J. Neurophysiol.* **51,** 90–112.
18. Freeman, W. J. (1979) *Biol. Cybern.* **35,** 21–37.
19. Finette, S., Harth, E. & Csermely, T. J. (1978) *Biol. Cybern.* **30,** 231–240.
20. Toyama, K., Kimura, M. & Tanaka, K. (1981) *J. Neurophysiol.* **46,** 202–213.
21. Gilbert, C. D. (1983) *Annu. Rev. Neurosci.* **6,** 217–247.
22. Martin, K. A. C. & Whitteridge, D. (1984) *J. Physiol. (London)* **353,** 463–504.
23. von Seelen, W., Mallot, H. A. & Giannakopoulos, F. (1987) *Biol. Cybern.* **56,** 37–49.
24. Ferster, D. (1986) *J. Neurosci.* **6(5),** 1284–1301.
25. Edelman, G. M. (1978) *The Mindful Brain* (MIT Press, Cambridge, MA).
26. Pearson, J. C., Finkel, L. H. & Edelman, G. M. (1987) *J. Neurosci.* **7(12),** 4209–4223.
27. Gray, C. M. & Singer, W. (1988) *ENA Abstr.* 11/86.4.
28. Singer, W., Gray, C. M., Engel, A. & König, P. (1988) *Neurosci. Abstr.* 14/362.13.